U. of Iowa 93-21

THE FINE STRUCTURE OF LANGMUIR WAVES OBSERVED UPSTREAM OF THE BOW SHOCK AT VENUS

by

G. B. Hospodarsky[1], D. A. Gurnett[1], W. S. Kurth[1],

M. G. Kivelson[2], R. J. Strangeway[2], and S. J. Bolton[3]

March 1994

[1]Department of Physics and Astronomy, The University of Iowa, Iowa City, IA 52242

[2]Institute of Geophysics and Planetary Physics, University of California, Los Angeles, CA 90024

[3]Jet Propulsion Laboratory, 4800 Oak Grove Drive, Pasadena, CA 91109

ABSTRACT

Highly structured Langmuir waves, also known as electron plasma oscillations, have been observed in the foreshock of Venus using the plasma wave experiment on the Galileo spacecraft during the gravity assist flyby on February 10, 1990. The Galileo wideband sampling system provides digital electric field waveform measurements at sampling rates up to 201,600 samples per second, much higher than any previous instrument of this type. The main Langmuir wave emission band occurs near the local electron plasma frequency, which was approximately 43 kHz. The Langmuir waves are observed to shift above and below the plasma frequency, sometimes by as much as 20 kHz. The shifts in frequency are closely correlated with the downstream distance from the tangent field line, implying that the shifts are controlled by the electron beam velocity. Considerable fine structure is also evident, with time scales as short as 0.15 milliseconds, corresponding to spatial scales of a few tens of Debye lengths. The frequency spectrum often consists of beat-type waveforms, with beat frequencies ranging from 0.2 to 7 kHz, and in a few cases, isolated wavepackets. The peak electric field strengths are approximately 1 mV/m. These field strengths are too small for strongly nonlinear processes to be important. The beat-type waveforms are suggestive of a parametric decay process.

I. INTRODUCTION

A region of strong Langmuir wave emissions was observed upstream of Venus' bow shock using the Galileo plasma wave experiment during the gravity assist flyby of Venus on February 10, 1990. These Langmuir waves were most likely produced by energetic electrons streaming into the solar wind from the bow shock, similar to the process by which Langmuir waves are generated upstream of the Earth's bow shock [Scarf et al., 1971]. Magnetic field-aligned electron fluxes propagating upstream from the bow shock to the spacecraft at energies above ~ 100 eV have been reported by the Galileo plasma instrument [Frank et al., 1991]. It is well known that electron beams can produce Langmuir waves by a process known as the beam-plasma instability [Bohm and Gross, 1949]. As the electrons stream along the interplanetary magnetic field lines, the solar wind convects the particles downstream as shown in Figure 1. Due to time-of-flight effects, only the highest energy (fastest) electrons can reach the spacecraft, thereby forming a beam [Filbert and Kellogg, 1979]. The electrons originating from the tangent point with the highest energy define a region called the electron foreshock (see Figure 1). One method of characterizing the location of the spacecraft in relation to the foreshock region is via a characteristic distance, D, called the depth parameter. The depth parameter is defined as the distance along the solar wind flow direction from the tangent magnetic field line to the spacecraft, as shown in Figure 1. The depth parameter is positive for spacecraft locations downstream of the electron foreshock boundary, and negative for locations upstream of the boundary. For a given depth parameter, only electrons with a velocity above a certain critical velocity can reach the spacecraft. The critical velocity can be determined from

the equation $v_c = d\ v_{sw}/D$ [Filbert and Kellogg, 1979] where v_c is the critical velocity, d is the distance along the tangent field line from the tangent point to the spacecraft, v_{sw} is the solar wind velocity, and D is the depth parameter. Electrons with velocity less than this critical velocity will be convected downstream before reaching the spacecraft.

Considerable effort has gone into explaining the observed characteristics of Langmuir waves. One of the areas of greatest interest, especially in association with Type III radio bursts, is the interaction of the Langmuir waves and the electron beam. The main issue involves the mechanism that allows the electron beam to propagate over large distances, much larger than allowed by a simple linear theory. Some of the mechanisms that have been proposed to limit the strength of the interaction include scattering by thermal fluctuations [Kaplin and Tsytovich, 1968], parametric and modulational decay instabilities [Papadopoulos et al., 1974; Fried et al., 1976; Bardwell and Goldman, 1976; Goldstein et al., 1979; Smith et al., 1979; Freund and Papadopoulos, 1980; Lin et al., 1986; Cairns and Robinson, 1992; Robinson et al., 1993], strongly nonlinear processes, such as soliton collapse [Zakharov, 1972; Galeev et al., 1975; Nicholson et al., 1978; Goldman, 1984; Shapiro and Shevchenko, 1984; Robinson and Newman, 1991], and the stochastic-growth model [Robinson, 1992; Robinson et al., 1992, 1993]. All these mechanisms shift the Langmuir waves out of resonance with the beam, which limits the growth of electric fields sufficiently to prevent the disruption of the beam. Another property which has received a great deal of attention [Gurnett et al., 1981; Etcheto and Faucheux, 1984; Fuselier et al., 1985; Lacombe et al., 1985; Cairns, 1987; Dum, 1990a, 1990b, 1990c] is the large spreading in frequency of the Langmuir waves observed in electron foreshock regions. Frequency spreading is also not predicted by the simple linear theory.

Scarf et al. [1980] and Crawford et al. [1990, 1991, 1993a, 1993b] using data from an electric field detector flown on the Pioneer Venus Orbiter have studied Langmuir waves upstream of the bow shock of Venus. These studies have shown that the characteristics of the Langmuir waves are very similar to the Langmuir waves observed upstream from the Earth's bow shock. The Langmuir waves are polarized with the wave electric field parallel to the static magnetic field, and are observed only when the spacecraft is magnetically connected to the bow shock. The peak electric field intensities are similar to Langmuir wave intensities observed upstream of the Earth's bow shock.

The Galileo spacecraft was launched on October 18, 1989, on a rather long and circuitous trip to Jupiter, which included a gravity assist flyby of Venus, and two flybys of Earth [Johnson et al., 1992]. The flyby of Venus provided an opportunity to capture high-time resolution measurements in the vicinity of Venus, with much higher resolution than provided by any previous instrument of this type. The measurements described here are from the plasma wave (PWS) and the magnetometer (MAG) experiments. The Galileo plasma wave experiment has several new capabilities, the most important of which is a high-rate sampling system that provides digital measurements of wideband electric and magnetic field waveforms at sampling rates of up to 201,600 samples per second. The high sampling rate allows Langmuir waves, and many other instabilities, to be resolved on the smallest time scale of physical interest, which is on the order of the electron plasma period, f_{pe}^{-1}. For a description of the Galileo plasma experiment, see Gurnett et al. [1992]. For a description of the Galileo magnetometer experiment, see Kivelson et al. [1992].

II. DESCRIPTION OF THE EVENT

The Langmuir waves presented here were observed by the Galileo plasma wave experiment on February 10, 1990. For a review of the initial Galileo Venus observations, see Kivelson et al. [1991], Gurnett et al. [1991], Williams et al. [1991], and Frank et al. [1991]. The interval over which the plasma wave experiment captured data at Venus was well positioned to observe the upstream Langmuir waves. Figure 2 shows the frequency-time spectrograms of the electric and magnetic field intensities obtained from the medium- and low-frequency receivers, which provide low-rate measurements in 116 channels from 5 Hz to 160 kHz. Four bow shock crossings determined by the magnetometer experiment [Kivelson et al., 1991] are shown by arrows at the top of Figure 2, along with the plasma region the spacecraft was in (solar wind or magnetosheath). The slight offset of the arrows from the increase in the electric and magnetic field noise levels in the spectrogram is due to the sweep time of the receivers and the size of the pixels. The multiple shock crossings are caused by the bow shock moving back and forth over the spacecraft [Kivelson et al., 1991]. The Langmuir waves can be seen in the upper panel (electric field spectrum) starting at about 0450 UT, in the 10 to 50 kHz frequency band. A weak Langmuir wave signal can also be seen between the shocks, from about 0440 to 0447 UT, also in the 10 to 50 kHz frequency band. At least two types of oscillations can be seen, one consisting of a nearly steady line at a frequency of about 43 kHz, which is believed to be the electron plasma frequency, f_{pe}, and a second component that is shifted both downward and upward in frequency from f_{pe}. The identification of the steady line at 43 kHz as the electron plasma frequency is in good agreement with the Galileo plasma instrument, which gave an

electron density of 22 cm^{-3}, which corresponds to a plasma frequency of 42 kHz for the time interval from 0448 to 0638 UT [Frank et al., 1991]. The 43-kHz component is most easily observed after the last shock crossing, starting at approximately 0450 UT and continuing sporadically until approximately 0525 UT. A very weak 43-kHz signal can also be seen between the two magnetosheath crossings, from about 0441 to 0444 UT. The upshifts and downshifts in frequency are most easily observed from approximately 0450 to 0502 UT, from 0505 to 0512 UT, and at 0524 UT.

III. WIDEBAND SPECTRUMS AND WAVEFORMS

The structure of the Langmuir waves can be observed in much greater detail using data from the wideband waveform receiver. The wideband receiver provides 4-bit samples of the electric field waveform at a variety of sampling rates. During the Venus flyby, the waveform receiver was operated in a duty cycle mode of operation at a sampling rate of 201,600 samples per second. The bandwidth of the anti-aliasing filter ahead of the analog-to-digital converter was selected to be 80 kHz. This mode of operation provides regularly spaced blocks of waveform data separated by gaps of constant duration. Data blocks of two different lengths were received during the Venus flyby. The majority of the data consists of blocks of 128 contiguous samples lasting 0.63 ms. Approximately 28 minutes of this "low" resolution data was recorded. Two longer length data blocks of approximately 78 seconds each were also recorded, one near the beginning of the measurement period, and the other at the end. This "high" resolution data consisted of blocks of 1576 contiguous samples lasting 7.82 ms. One waveform block is captured every 66.67 ms, for both cases, with a gap of 66.04 and 58.85 ms, respectively, between successive waveforms. To increase the dynamic range of the receiver (4-bit digitization provides a dynamic range of $\sim$24 db), an automatic gain control (AGC) circuit was used to control the amplitude of the signal into the analog-to-digital converter. The time constant of the AGC is approximately 0.1 seconds. The AGC value is sampled once every 2.67 seconds, which allows the absolute field strengths to be determined every 2.67 seconds with a 0.1-second interval.

One way to display the waveform data is to Fourier transform each of the waveform blocks, and then plot the sequence of transform amplitudes in the form of a frequency-time spectrogram. An example of such a spectrogram is shown in Figure 3. The spectrogram shows a 50-second interval of the high-resolution waveforms (7.82 ms blocks). The Langmuir waves can be most easily seen as the bursty signals that start approximately 12 seconds into the spectrogram. A weak signal at approximately 43 kHz can also be observed a few seconds before the onset of the much stronger emission. The Langmuir waves show large upshifts and downshifts in frequency from the electron plasma frequency, which was estimated to be approximately 43 kHz during this period. The upshifts and downshifts can be as large as 20 kHz. The Langmuir waves also show extremely rapid temporal variations, many with time scales smaller than the time between successive waveform blocks (66.67 ms).

The top panel of Figure 4 shows a frequency-time spectrogram of the low-resolution waveforms (0.63 ms blocks). This spectrogram shows the entire low-resolution data set. Note that the time axis is now in minutes, and the total interval displayed is 30 minutes, from 0435 to 0505 UT. The observed signals are composed of two components, a weak narrowband component near the plasma frequency, and a stronger broader bandwidth component which shows large upshifts and downshifts in frequency. The middle panel of Figure 4 shows the depth parameter (see Figure 1) as inferred from the measured solar wind magnetic field [Kivelson et al., 1991]. Note that the depth and up distance from the caption of Figure 5 [Kivelson et al., 1991] is incorrect. Depth is defined as positive when the spacecraft is antisunward of the foreshock boundary, and up distance is negative in the antisunward direction from the tangent point.

The variability in the depth parameter was estimated by varying the terminator shock distance. Using as an upper limit the range of 0.1 R_v as a function of θ_{bn} found by Zhang et al. [1991] for the terminator crossing distances, the eccentricity and semi-latus rectum of the shock model was modified in order to maintain a fixed sub-polar distance of the shock. The shock model terminator distance ranged from 2.309 to 2.409 R_v, corresponding to eccentricities of 0.925 to 0.995. The referenced shock has a terminator distance of 2.359 R_v, eccentricity of 0.96, sub-polar distance of 1.425 R_v, and focus offset of 0.4 R_v. The changing of the shock shape has the largest effect on the depth parameter for increasing distance downstream of the sub-solar point. The projected field line encounters the shock around $x = -5$ R_v when the depth is near zero in Figure 4, and the variability is largest here. Furthermore, in determining the range, this analysis assumes that θ_{bn} varies from 0° to 90°, but since the field is nearly tangent to the shock surface, $\theta_{bn} \sim 90°$ for depth $\sim$ 0. Thus the errors bars give an upper limit to the range in depth.

As can be seen, the magnitude of the depth parameter and the shifts in the frequency of the Langmuir waves are correlated. The correlation is especially evident after 0450 UT. As the depth parameter increases from approximately 0450 to 0453 UT, the Langmuir waves shift downward in frequency. From approximately 0453 to 0500 UT, the downshifted Langmuir waves drift up in frequency as the magnitude of the depth parameter decreases. From approximately 0500 to 0503 UT, the depth parameter is small (~ 1 R_v) and the Langmuir waves shift up in frequency. The correlation before 0450 UT is not as good. During this period, the uncertainties in the depth parameter and the spacecraft crossing in and out of the bow shock make it more difficult to compare the depth parameter and the Langmuir waves. The correlation of the depth parameter with the downshifts and upshifts in frequency has also been observed at

the Earth, and has been determined to be related to the speed of the electron beams producing the Langmuir waves [Etcheto and Faucheux, 1984; Fuselier et al., 1985; Lacombe, 1985].

The origin of the narrowband emission near the plasma frequency, for the period from approximately 0441 to 0446 UT and 0452 to 0459 UT, is not as well understood. The low intensity and steadiness of this emission during the period of rather large variations of the depth parameter is suggestive of thermally excited Langmuir waves [Meyer-Vernet and Perche, 1989]. Meyer-Vernet and Perche [1989] present analytical expressions and numerical results of the thermally excited Langmuir waves for a range of plasma conditions and ratios of the effective antenna length to the Debye length (L/λ_D). Their spectrum of thermally excited Langmuir waves (their Figure 8) produced by a bi-Maxwellian plasma with a ratio of the temperature of the hot component to the cold component = 100, and with $L/\lambda_D = 1$, has the same basic shape as the observed narrowband emission, but their predicted electric field intensities are smaller than the observed electric field intensities by approximately a factor of ten. Also, four periods (0439-0441 UT, 0447-0448 UT, 0449-0450 UT, and 0502-0503 UT) can be observed in Figure 4 where the narrowband emission disappears as the depth parameter goes to zero, which corresponds to Galileo leaving the foreshock. The first two periods correspond to times when Galileo entered the magnetosheath [Kivelson et al., 1991]. The absence of a signal during these periods can be explained by the decrease in the gain of the wideband receiver due to the strong broadband low-frequency signals that are present in this region (see Figure 2). During the last two intervals, Galileo is upstream of the tangent field line and no longer in the foreshock region (it is believed from the characteristics of the electric and magnetic field spectrum from Figure 2 that the last period corresponds to Galileo briefly exiting the foreshock, even though the depth parameter is still positive). This disappearance of the narrowband signal as Galileo exits the

foreshock is not expected in this region. The model of the thermally excited Langmuir emissions assumes only a bi-Maxwellian plasma and does not take into account the presence of an electron beam. The discrepancy of the observed emission with the theory could possibly be removed by redoing the analysis of Meyer-Vernet and Perche [1989] for the specific conditions encountered by Galileo during this period. Particularly, a detailed analysis of the Galileo antenna configuration (the Galileo antenna is not a simple linear wire dipole antenna), using the actual L/λ_D value of ~ 0.4, and using the actual plasma parameters and electron distribution functions found in the foreshock region and in the solar wind upstream of the foreshock boundary at Venus.

An alternative explanation of the origin of the narrowband emissions has been proposed by Onsager and Holzworth [1990]. They suggest that long wavelength, weakly damped Langmuir waves generated at the foreshock boundary are convected downstream by the solar wind. Their measurements at the Earth's foreshock using the AMPTE spacecraft showed a spectrogram (their Figure 1) that is very similar to the spectrogram in the top panel of Figure 4, but the electric field intensity of their emission at the plasma frequency was usually larger than the electric field intensity of the downshifted emissions. The opposite was observed at Venus. The electric field intensity of the downshifted emissions observed upstream of Venus was usually larger than the emission at the plasma frequency.

A similar model of downstream waves based on convection from the foreshock boundary has been proposed by Robinson and Newman [1991]. In their model, wave packets are formed near the foreshock boundary by nonlinear strong-turbulence effects. These wave packets convect downstream with the solar wind while collapsing to short scale lengths and high electric field intensities, much higher than the electric fields observed at Venus. This model was developed

to account for the distribution of the most intense plasma waves observed at the Earth's electron foreshock, and does not predict the weak emission that is observed at Venus.

A fourth possible explanation for the narrowband emissions is that high-speed electron beams are present at the same time as the slow-speed electron beams. The high-speed beam could produce the emission near the plasma frequency, and the slow beam could produce the downshifted emissions. Further work is required to determine the exact process, or processes, that produce the narrowband emission near the plasma frequency.

To examine the fine structure of the Langmuir waves, the individual waveform blocks were studied. Approximately 28,000 waveform blocks were captured by the wideband waveform receiver, of which approximately 2360 were 7.82 ms blocks, and 25,800 were 0.63 ms blocks. Figure 5 shows four waveform blocks from the high-resolution mode (7.82 ms). As can be seen, the waveforms show considerable variations. The high-frequency quasi-sinusoidal waveforms evident in each of the plots are the Langmuir wave oscillations. The most striking feature is the beat-type waveforms. Panel (a) and (d) show a string of wave packets that are suggestive of a beat between two nearly monochromatic waves of comparable amplitude. Further evidence of the beat hypothesis can be obtained from the spectrum of the beat-type waveforms. Figure 6 shows the spectrum of the waveform from panel (d). Two distinct frequency components, one at approximately 45.5 kHz and the other at approximately 48.3 kHz are observed. The frequency difference of these two signals agrees with the observed beat frequency ($\sim$2.8 kHz). The frequency of the beat pattern varies throughout the data set, from approximately 0.2 to 7 kHz. Beat frequencies below 0.2 kHz probably occur, but the gaps between waveform blocks prevent any determination of lower frequency characteristics. Panel (b) shows a more chaotic waveform. A weak beat pattern can usually be observed in this type

of waveform, but it is not as evident as cases similar to panels (a) and (d). Panel (c) suggests a beat-like waveform of a lower frequency, or possibly an isolated wavepacket. The limited length of the waveform blocks and the 58.85 ms data gap between blocks prevents the determination of the exact characteristics of this waveform.

IV. ELECTRIC FIELD AMPLITUDES

The most important parameter for determining the role of nonlinear processes is the electric field amplitude. If the ratio of the electric field energy density to the plasma energy density, $\epsilon_0 E^2/(8\pi n\kappa T)$, is greater than $(k\lambda_D)^2$, then a strongly nonlinear process, such as soliton collapse can occur. However, the electric field amplitude is difficult to measure for bursty signals. The low-rate spectrum analyzer has an integration time constant of 50 ms which is too long to provide an accurate determination of the amplitude of the millisecond bursts. The high-rate waveform measurements do not have this limitation. However, the waveform measurements have an automatic gain control. As the gain of the receiver varies in time, absolute amplitude measurements can only be obtained at times when the AGC value is sampled. Even then, there is a risk that the waveform may be strongly clipped, which prevents an accurate measurement. The AGC value is sampled every 2.67 seconds, and the AGC has a time constant of approximately 0.1 seconds, which allows the absolute electric field strengths to be determined every 2.67 seconds with a 0.1-second interval around the time the AGC sample is taken. This corresponds to approximately 6% of the available waveform blocks. During the Venus flyby, AGC values were available for 1770 waveform blocks, and of these, 601 had distinguishable Langmuir wave emissions.

Each of the 601 waveform blocks were examined to determine the peak electric field amplitude. If the waveform was not clipped, the peak amplitude was read directly from the plot. If the waveform was clipped, the peak amplitude was estimated by extrapolating the envelope of the waveform beyond the boundary of the plot. For a more detailed description of the

method of deriving amplitudes from the waveform data, see Gurnett et al. [1993]. Approximately 9% of the 601 waveforms that have corresponding AGC values were clipped in some manner, but none of these waveforms were so severely clipped that the peak amplitude could not be estimated by extrapolating the waveform envelope beyond the plot. The results of this survey are shown in Figure 7. As can be seen, the largest peak electric field amplitude was a little over 1 mV/m, which corresponds to an energy density ratio of approximately 10^{-8}. The majority of the amplitudes ranged between 0.003 and 0.1 mV/m (energy density ratios of 10^{-13} to 10^{-11}). These results are in good agreement with the Pioneer Venus electric field measurements reported by Crawford et al. [1990]. The flattening of the distribution at approximately 0.05 mV/m, and the sharp drop off in the number of events below 0.01 mV/m is probably caused by the background noise level (due to the receiver noise level and other low-level signals), which makes it difficult to measure weak field strengths, especially for the low-resolution waveforms (0.63 ms blocks).

The bottom panel of Figure 4 shows the variation over time of the peak electric field strength of the Langmuir waves shown in Figure 7. The largest amplitudes tend to occur during periods of small depth parameters (for example 04:38.5, 04:47 to 04:51 and 05:02 UT). These periods corresponds to times when the spacecraft is near the foreshock boundary. This correlation agrees with results obtained at Venus [Crawford et al., 1990, 1991] and at the Earth [Filbert and Kellogg, 1979; Etcheto and Faucheux, 1984; Fuselier et al., 1985; Lacombe et al., 1985] which showed that the largest electric field amplitudes were observed near the foreshock boundary.

V. DISCUSSION

This paper has used the very high-resolution waveform measurements captured by the Galileo plasma wave experiment to describe the fine structure of Langmuir waves observed in the solar wind upstream of the bow shock of Venus. The Langmuir waves contain both long-time scale structure (the downshifts and upshifts in frequency) and short-time scale structure (beat-type wave packets). The shortest time scales consist mainly of highly coherent beat-type waveforms, with beat frequencies ranging from approximately 0.2 to 7 kHz. Little structure is observed at time scales less than about 0.15 ms. If we assume that the structures are convected by the spacecraft at the solar wind speed ($\sim$450 km/s), this time scale would correspond to a spatial scale of $\sim$65 meters. This spatial cutoff is probably related to the Debye length, which is given by $\lambda_D = 0.069\ (T/n)^{1/2}$ m, where T is in °K and n is in cm^{-3}. Using the solar wind parameters from Frank et al. [1991] (n = 22 cm^{-3}, v = 450 km/s, and T = 3.1 x 10^5 °K), λ_D is found to be 8.2 m. By dividing λ_D by the solar wind speed, 100 λ_D is found to be 1.82 ms which is shown at the top of Figure 5. The short scale cutoff of 0.15 ms corresponds to a spatial scale of approximately 8 Debye lengths.

The very fine structure of the waveforms is suggestive of a nonlinear process. Similar waveforms have been observed in the electron foreshock of Jupiter [Gurnett et al., 1981] and of Earth [Hospodarsky et al., 1991], and in association with a Type III radio burst [Gurnett et al., 1993]. The isolated wavepackets are suggestive of a strong nonlinear process, such as soliton collapse. However, the field strengths usually are too small to support this conclusion. To determine if the fine structure of the Langmuir waves observed at Venus is caused by a

strong nonlinear process, the ratio of the electric field energy density, $E^2/8\pi$, to the plasma energy density, $n\kappa T$ was calculated. If $\epsilon_0 E^2/(n\kappa T) > (k\lambda_D)^2$ then the interaction is considered strong, otherwise it is a weak process. Using the solar wind parameters from above and taking $k = 2\pi/L$, where $L = 8\ \lambda_D$ is the smallest scale size for the wave packets, the threshold for a strong nonlinear process is approximately 3.6 V/m. This threshold is over three thousand times larger than any of the measured values. If an electric field of 1 mV/m is assumed, which is the largest field that was measured, a scale length of approximately 29,000 λ_D, or 528 ms, is needed. It is possible that some of the waveform blocks that do not have corresponding AGC values could have a much higher amplitude than 1 mV/m, but it is doubtful that any have amplitudes as large as 3.6 V/m. Amplitudes of this magnitude would severely clip and distort the waveform receiver, and no severe distortion of this type was observed.

The beat-type waveforms are strongly suggestive of two waves of comparable amplitude, but slightly different frequency interfering with each other. One possible explanation is that the beat-type waveforms are Langmuir waves excited by electron beams of different velocities. Variations of the electron beam velocities have been proposed to explain the observed downshifts and upshifts in frequency [Fuselier et al., 1985; Cairns, 1987]. However, this explanation does not explain the many cases where the two waves are of comparable amplitudes. Random superposition of wave packets from waves excited by different velocity beams would not be expected to have the same amplitude. Different electron beam velocities may account for some of the fine structure that is observed. However, it is unlikely that it accounts for all of the beat-like waveforms.

A more likely cause of many of the beat-type waveforms is a weak-turbulence process. The two most likely processes are scattering of Langmuir waves off thermal ions and a

parametric decay process, specifically Langmuir wave decay. Scattering off thermal ions involves a Langmuir wave (ω, $\mathbf{k}$) being scattered off a plasma ion, producing a new Langmuir wave (ω_1, $\mathbf{k}_1$). The parametric decay process involves an initial Langmuir wave, ω_1, which decays into a second Langmuir wave, ω_2, and a low-frequency wave, ω_L. The process must conserve energy, $\omega_1 = \omega_2 + \omega_L$, and momentum, $\mathbf{k}_1 = \mathbf{k}_2 + \mathbf{k}_L$. These two processes do not require large field strengths, and both predict beat-type waveforms. Recent results by Cairns [1993] has shown that for typical solar wind conditions and Langmuir wave amplitudes, the Langmuir decay process $L \rightarrow L' + S$ should dominate the process of scattering off thermal ions.

Cairns and Robinson [1992] have developed a theory based on Langmuir wave decay that predicts the electron beam speed for a observed beat frequency, after taking into account the Doppler shift due to the solar wind-spacecraft relative motion. Using the parameters determined by the magnetometer experiment [Kivelson et al., 1991] for the period of the high-resolution waveforms (Figure 3), and assuming beat frequencies ranging from 0.2 to 7 kHz, this theory predicts beam speeds of 91 x 10^6 to 4.5 x 10^6 m/s. These predicted beam speeds agree very well with the magnetic field aligned electron fluxes of 100 to 1000 eV (6 x 10^6 to 20 x 10^6 m/s) measured by the plasma instrument [Frank et al., 1991].

Langmuir wave decay predicts that a low-frequency wave, probably an ion acoustic wave, should be observed. Even though there is no evidence of low-frequency waves related to Langmuir waves in Figure 3, an examination of the individual spectra of beat-type waveforms often shows a weak low-frequency signal. Figure 8 shows the spectrum of the waveform in panel (b) of Figure 5. As can be seen, there are two main peaks, one centered at approximately 46 kHz, which is near the plasma frequency, and another that is upshifted in frequency, and centered at approximately 53 kHz. Each of the two main signals is broad in frequency and

contains a great deal of structure. There is also a series of weak signals located from a few hundred Hz to about 9 kHz. The broadband signal located from approximately 6 to 8 kHz is the approximate frequency difference of the two main signals, and is in good agreement with the beat frequency observed in the waveform ($\sim$7 kHz). The low-frequency signals, especially the signals located at the observed beat frequencies, are strongly suggestive of the low-frequency ion acoustic waves predicted above. These signals are often very weak and do not appear in every beat-type waveform spectrum, which may explain why they are not observed in Figure 3. Though these features suggest a parametric decay process, further work and analysis are needed to confirm these results.

ACKNOWLEDGEMENTS

The authors would like to thank Larry Granroth and Janice Cook-Granroth for their efforts in carrying out the data processing. Useful discussions with Iver Cairns are also gratefully acknowledged. This research was supported by the Iowa Space Grant Consortium Fellowship program and by NASA through contract 958779 with the Jet Propulsion Laboratory. The magnetometer investigation is supported by NASA through contract 958694 with the Jet Propulsion Laboratory.

REFERENCES

Bardwell, S., and M. V. Goldman, Three-dimensional Langmuir wave instabilities in type III solar radio bursts, Astrophys. J., 209, 912, 1976.

Bohm, D., and E. P. Gross, Theory of plasma oscillations: A, Origin of medium-like behavior; B, Excitation and damping of oscillations, Phys. Rev., 75, 1851, 1949.

Cairns, I. H., A theory for the Langmuir waves in the electron foreshock, J. Geophys. Res., 92, 2329, 1987.

Cairns, I. H., When does the Langmuir wave decay dominate scattering of thermal ions?, EOS, 74, No. 43, 478, 1993.

Cairns, I. H. and P. A. Robinson, Theory for low-frequency modulated Langmuir wave packets, Geophys. Res. Lett., 19, 2187, 1992.

Crawford, G. K., R. J. Strangeway, and C. T. Russell, Electron plasma oscillations in the Venus foreshock, Geophys. Res. Lett., 17, 1805, 1990.

Crawford, G. K., R. J. Strangeway, and C. T. Russell, Variations in plasma wave intensity with distance along the electron foreshock boundary at Venus, Adv. Space Res., 11, (9)93, 1991.

Crawford, G. K., R. J. Strangeway, and C. T. Russell, VLF emissions in the Venus foreshock: Comparison with terrestrial observations, J. Geophys. Res., 98, 15305, 1993a.

Crawford, G. K., R. J. Strangeway, and C. T. Russell, VLF imagine of the Venus foreshock, in press Geophys. Res. Lett., 1993b.

Dum, C. T., Simulations of plasma waves in the electron foreshock: The generation of Langmuir waves by a gentle bump-on-tail electron distribution, J. Geophys. Res., 95, 8095, 1990a.

Dum, C. T., Simulations of plasma waves in the electron foreshock: The transition from reactive to kinetic instability, J. Geophys. Res., 95, 8111, 1990b.

Dum, C. T., Simulations of plasma waves in the electron foreshock: The generation of downshifted oscillations, J. Geophys. Res., 95, 8123, 1990c.

Etcheto, J., and M. Faucheux, Detailed study of electron plasma waves upstream of the Earth's bow shock, J. Geophys. Res., 89, 6631, 1984.

Filbert, P. C., and P. J. Kellogg, Electrostatic noise at the plasma frequency beyond the Earth's bow shock, J. Geophys. Res., 84, 1369, 1979.

Frank, L. A., W. R. Paterson, K. L. Ackerson, F. V. Coroniti, V. M. Vasyliunas, Plasma observations at Venus with Galileo, Science, 252, 1528, 1991.

Freund, H. P., and K. Papadopoulos, Oscillating two-stream and parametric decay instability in a weakly magnetized plasma, Phys. Fluids, 23, 139, 1980.

Fried, B. D., T. Ikemura, K. Nishikawa, and G. Schmidt, Parametric instabilities with finite wavelength pump, Phys. Fluids, 19, 1975, 1976.

Fuselier, S. A., D. A. Gurnett, and R. J. Fitzenreiter, The downshift of electron plasma oscillations in the electron foreshock region, J. Geophys. Res., 90, 3935, 1985.

Galeev, A. A., R. Z. Sagdeev, Yu. S. Sigov, V. D. Shapiro, and V. I. Shevchenko, Nonlinear theory for the modulational instability of plasma waves, Sov. J. Plasma Phys. Engl. Transl., 1, 5, 1975.

Goldman, M. V. Strong turbulence of plasma waves, Rev. Mod. Phys., 56, 709, 1984.

Goldstein, M. L., R. A. Smith, and K. Papadopoulos, Nonlinear stability of solar type III radio bursts, II, Application to observations near 1 AU, Astrophys. J., 234, 683, 1979.

Gurnett, D. A., J. E. Maggs, D. L. Gallagher, W. S. Kurth, and F. L. Scarf, Parametric interaction and spatial collapse of beam-driven Langmuir waves in the solar wind, J. Geophys. Res., 86, 8833, 1981.

Gurnett, D. A., W. S. Kurth, A. Roux, R. Gendrin, C. F. Kennel, and S. J. Bolton, Lightning and plasma wave observations from the Galileo flyby of Venus, Science, 253, 1522, 1991.

Gurnett, D. A., W. S. Kurth, R. R. Shaw, A. Roux, R. Gendrin, C. F. Kennel, F. L. Scarf, and S. D. Shawhan, The Galileo plasma wave investigation, Space Sci. Rev., 60, 341, 1992.

Gurnett, D. A., G. B. Hospodarsky, W. S. Kurth, D. J. Williams, and S. J. Bolton, The fine structure of Langmuir waves produced by a solar electron event, J. Geophys. Res., 98, 5631, 1993.

Hospodarsky, G. B., D. A. Gurnett, W. S. Kurth, and A. J. Bolton, High resolution measurements of Langmuir waves upstream of the Earth's bow shock, EOS, 72, No. 44, 390, 1991.

Johnson, T. V., C. M. Yeates, and R. Young, Space science reviews volume on Galileo mission overview, Space Sci. Rev., 60, 3, 1992.

Kaplan, S. A., and V. N. Tsytovich, Radio emission from beams of fast particles under cosmic conditions, Sov. Astron. Engl. Transl., 11, 956, 1968.

Kivelson, M. G., C. F. Kennel, R. L. McPherron, C. T. Russell, D. J. Southwood, R. J. Walker, C. M. Hammond, K. K. Khurana, R. J. Strangeway, P. J. Coleman, Magnetic

field studies of the solar wind interaction with Venus from the Galileo flyby, Science, 253, 1518, 1991.

Kivelson, M. G., K. K. Khurana, J. D. Means, C. T. Russell, and R. C. Snare, The Galileo magnetic field investigation, Space Sci. Rev., 60, 357, 1992.

Lacombe, C. A., A. Mangency, C. C. Harvey, and J. D. Scudder, Electron plasma waves upstream of Earth's bow shock, J. Geophys. Res., 90, 73, 1985.

Lin, R. P., W. K. Levedahl, W. Lotko, D. A. Gurnett, and F. L. Scarf, Evidence for nonlinear wave-wave interactions in solar type III radio bursts, Astrophys. J., 308, 954, 1986.

Meyer-Vernet N., and C. Perche, Tool kit for antennae and thermal noise near the plasma frequency, J. Geophys. Res., 94, 2405, 1989.

Nicholson, D. R., M. V. Goldman, P. Hoyng, and J. C. Weatherall, Nonlinear Langmuir waves during type III solar radio bursts, Astrophys. J., 223, 605, 1978.

Onsager, T. G. and R. H. Holzworth, Measurement of the electron beam mode in Earth's foreshock, J. Geophys. Res., 95, 1990.

Papadopoulos, K., M. L. Goldstein, and R. A. Smith, Stabilization of electron streams in type III solar radio bursts, Astrophys. J., 190, 175, 1974.

Robinson, P. A., Clumpy Langmuir waves in Type III radio sources, Sol. Phys., 139, 147, 1992.

Robinson, P. A. and D. L. Newman, Strong plasma turbulence in the Earth's electron foreshock, J. Geophys. Res., 96, 17733, 1991.

Robinson, P. A., I. H. Cairns, and D. A. Gurnett, Connection between ambient density fluctuations and clumpy langmuir waves in the Type III radio sources, Astrophys. J., 387, L101-L104, 1992.

Robinson, P. A., A. J. Willies, and I. H. Cairns, Dynamics of Langmuir and ion-sound waves in type III solar radio sources, Astrophys. J., 408, 720, 1993.

Scarf, F. L., R. W. Fredricks, L. A. Frank, and M. Neubauer, Nonthermal electrons and high frequency waves in the upstream solar wind, 1, Observations, J. Geophys. Res., 76, 5162, 1971.

Scarf, F. L., W. W. L. Taylor, C. T. Russell, and R. C. Elphic, Pioneer Venus plasma wave observations: The solar wind-Venus interaction, J. Geophys. Res., 85, 7599, 1980.

Shapiro, V. D., and V. I. Shevchenko, Strong turbulence of plasma oscillations, Basic Plasma Physics. Handbook of Plasma Physics, Vol. 2, ed. by A.A. Galeev and R.N. Sudan, North Holland, 123, 1984.

Smith, R. A., M. L. Goldstein, and K. Papadopoulos, Nonlinear stability of solar type III radio bursts, I, Theory, Astrophys. J., 234, 348, 1979.

Williams, D. J., R. W. McEntire, S. M. Krimigis, E. C. Roelof, S. Jaskulek, B. Tossman, B. Wilken, W. Stüdemann, T. P. Armstrong, T. A. Fritz, L. J. Lanzerotti, and J. G. Roederer, Energetic particles at Venus: Galileo results, Science, 203, 1525, 1991.

Zakharov, V. E., Collapse of Langmuir waves, Sov. Phys. JETP Engl. Transl., 35, 908, 1972.

FIGURE CAPTIONS

Figure 1. A sketch of the electron foreshock region of Venus. Electrons streaming from the bow shock along the magnetic field lines are convected downstream by the solar wind. These electron beams generate Langmuir waves by the beam-plasma instability. The depth parameter, D, is defined as the distance from the tangent magnetic field line to the spacecraft.

Figure 2. A frequency-time spectrogram of the electric and magnetic field intensities measured by the medium- and low-frequency spectrum analyzers. Four bow shock crossings and the plasma region the spacecraft was in are shown at the top of Figure 2. The Langmuir waves can be most easily seen after the last bow shock crossing, in the frequency band 10 to 50 kHz of the electric field spectrum (from Gurnett et al. [1991]).

Figure 3. A high-resolution frequency-time spectrogram of the Langmuir waves. The Langmuir waves show temporal structure down to the resolution of the Fourier transform (66.67 ms). Large upshifts and downshifts in the emission frequency compared to the plasma frequency ($\sim$43 kHz) are also observed (from Gurnett et al. [1991]).

Figure 4. The top panel is a high-resolution frequency-time spectrogram of the Langmuir waves. The middle panel is a plot of the depth parameter. A good correlation exists between the shifts in frequency of the Langmuir waves and the depth parameter value. The bottom panel is a plot of the maximum peak electric field

amplitude of the waveform blocks. The largest fields are observed when the spacecraft is near the tangent magnetic field line (small D).

Figure 5. A sampling of the Langmuir emission electric field waveforms. Note the considerable temporal structure down to time scales of 0.15 ms.

Figure 6. The spectrum of the waveform from panel (d) of Figure 5. The two distinct signals at approximately 45.5 kHz and 48.3 kHz are evidence that the beat-type waveforms are caused by two waves of comparable amplitude and slightly different frequency beating with each other.

Figure 7. The number of waveform blocks as a function of the peak electric field strength.

Figure 8. The spectrum of the waveform from panel (b) of Figure 5. Note the weak low-frequency signals located from a few hundred Hz to approximately 9 kHz. These low-frequency signals are suggestive of the low-frequency ion acoustic waves predicted by parametric decay.

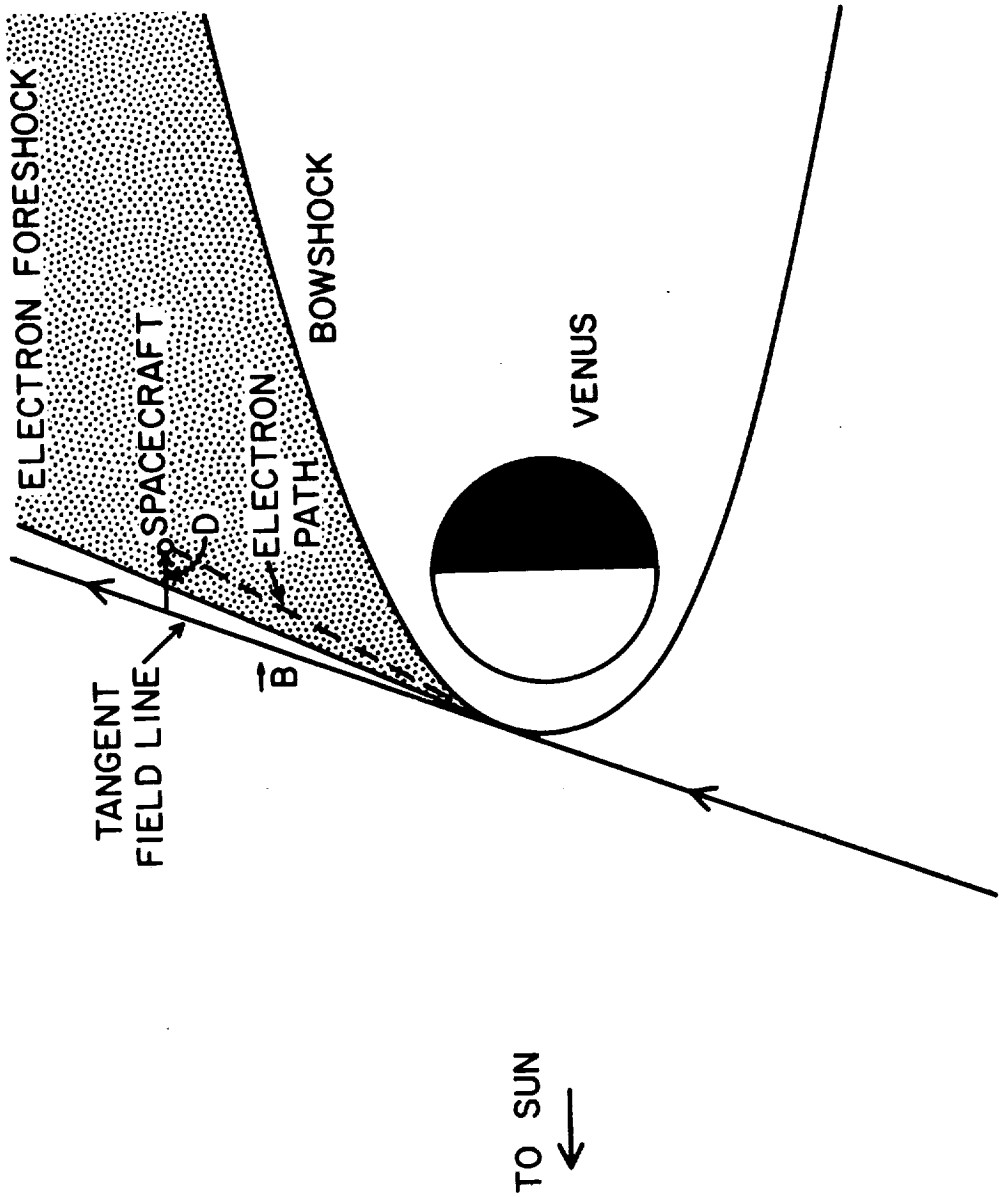
A-G93-62-2
ELECTRON FORESHOCK
SPACECRAFT
D
ELECTRON PATH
BOWSHOCK
VENUS
TANGENT FIELD LINE
B
TO SUN

Figure 1

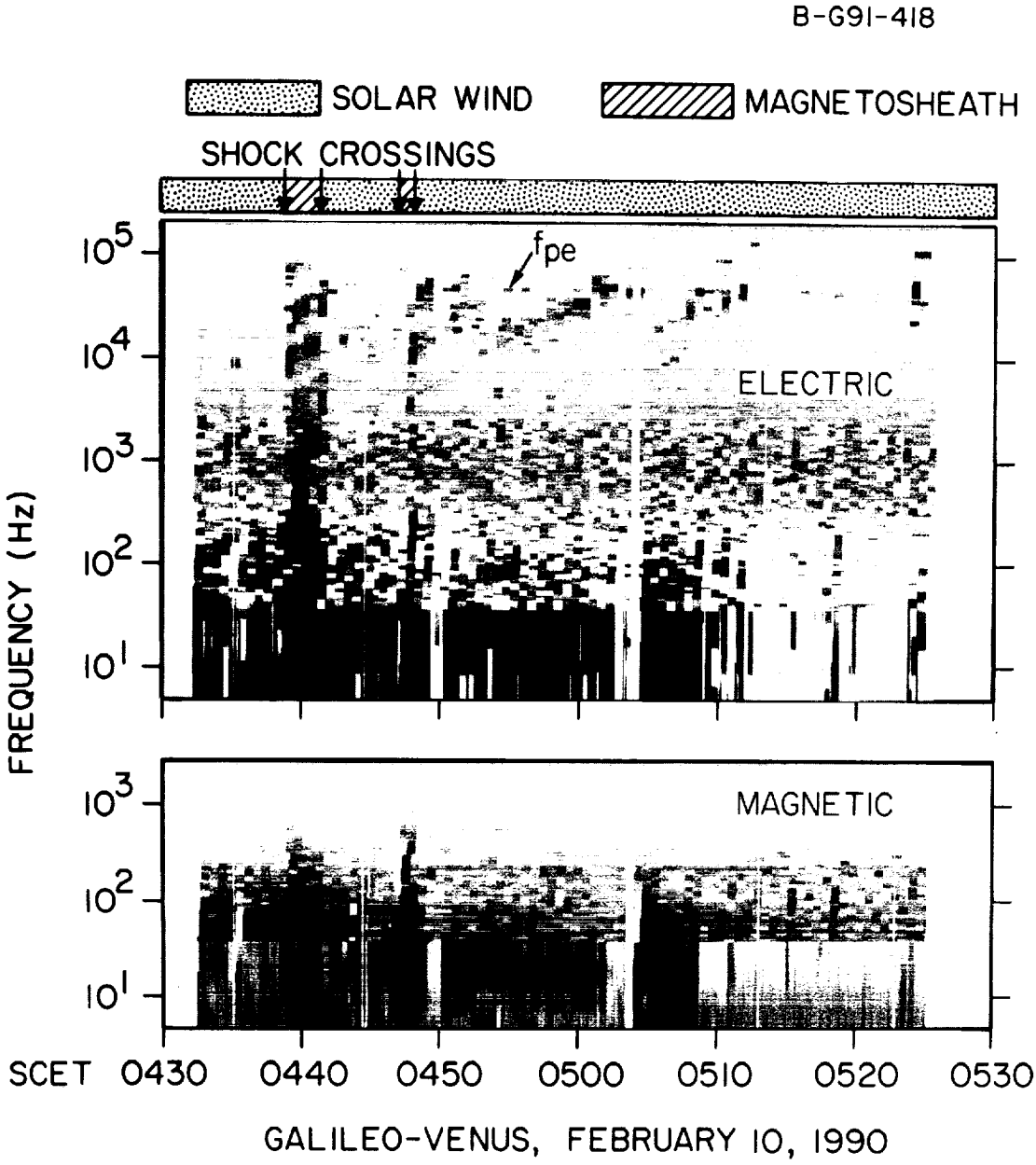
B-G91-418
SOLAR WIND
MAGNETOSHEATH
SHOCK CROSSINGS
f_{pe}
ELECTRIC
MAGNETIC
FREQUENCY (Hz)
10^5
10^4
10^3
10^2
10^1
10^3
10^2
10^1
SCET 0430 0440 0450 0500 0510 0520 0530
GALILEO-VENUS, FEBRUARY 10, 1990

Figure 2

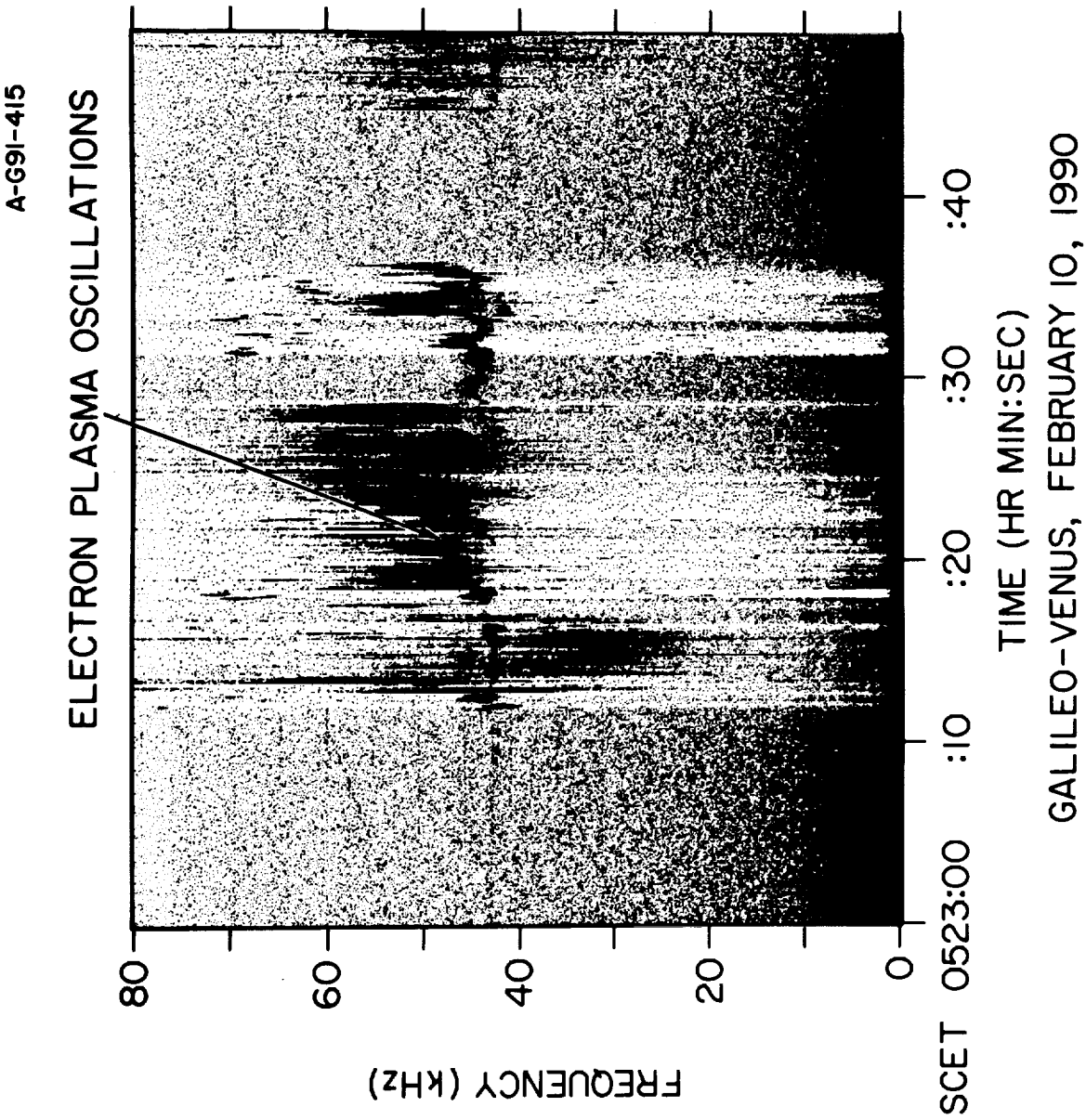
A-G91-415
ELECTRON PLASMA OSCILLATIONS
80
60
40
20
0
FREQUENCY (kHz)
SCET 0523:00
:10
:20
:30
:40
TIME (HR MIN:SEC)
GALILEO-VENUS, FEBRUARY 10, 1990

Figure 3

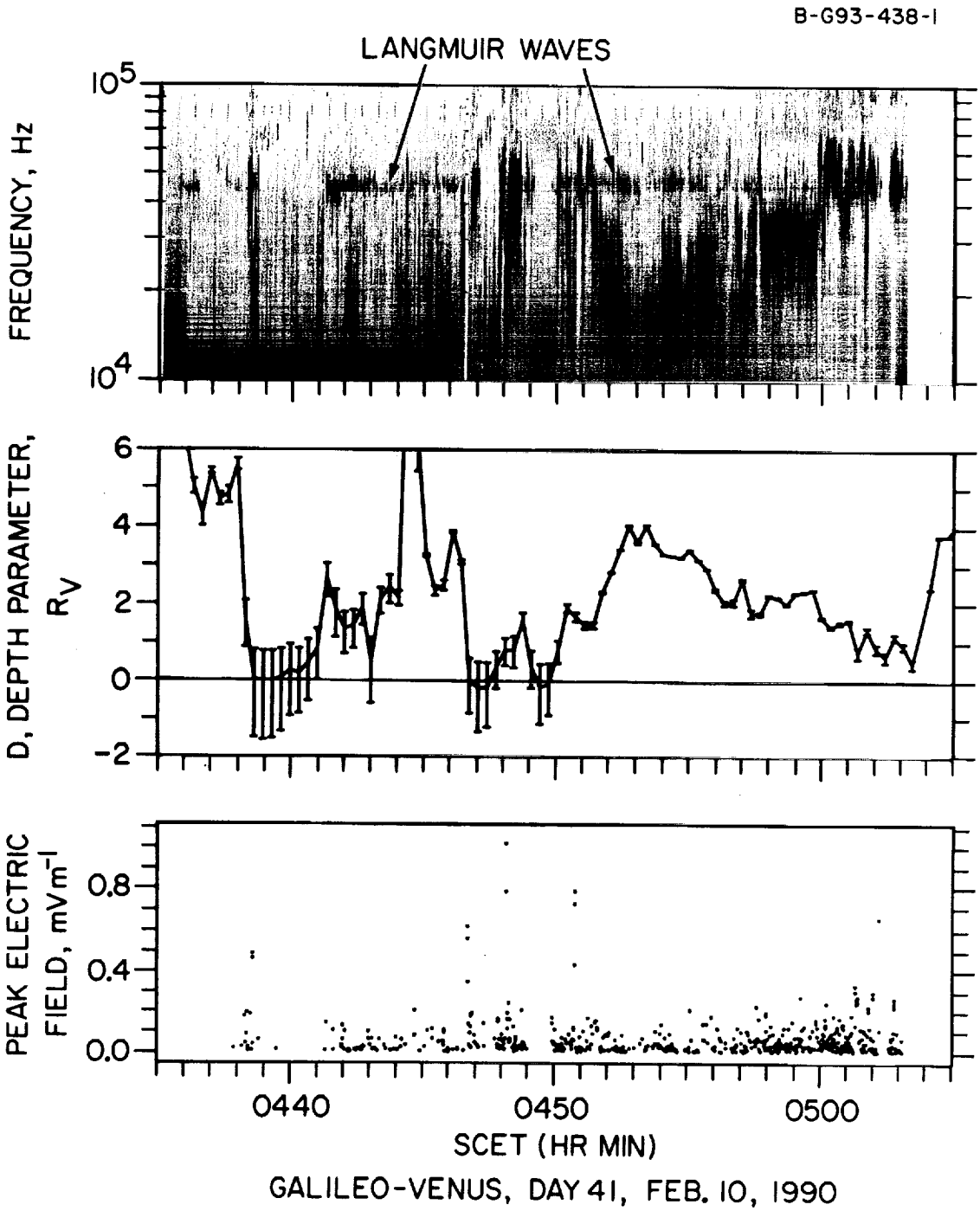
B-G93-438-1
LANGMUIR WAVES
FREQUENCY, Hz
10^5
10^4
D, DEPTH PARAMETER, R_V
6
4
2
0
-2
PEAK ELECTRIC FIELD, mVm^{-1}
0.8
0.4
0.0
0440
0450
0500
SCET (HR MIN)
GALILEO-VENUS, DAY 41, FEB. 10, 1990

Figure 4

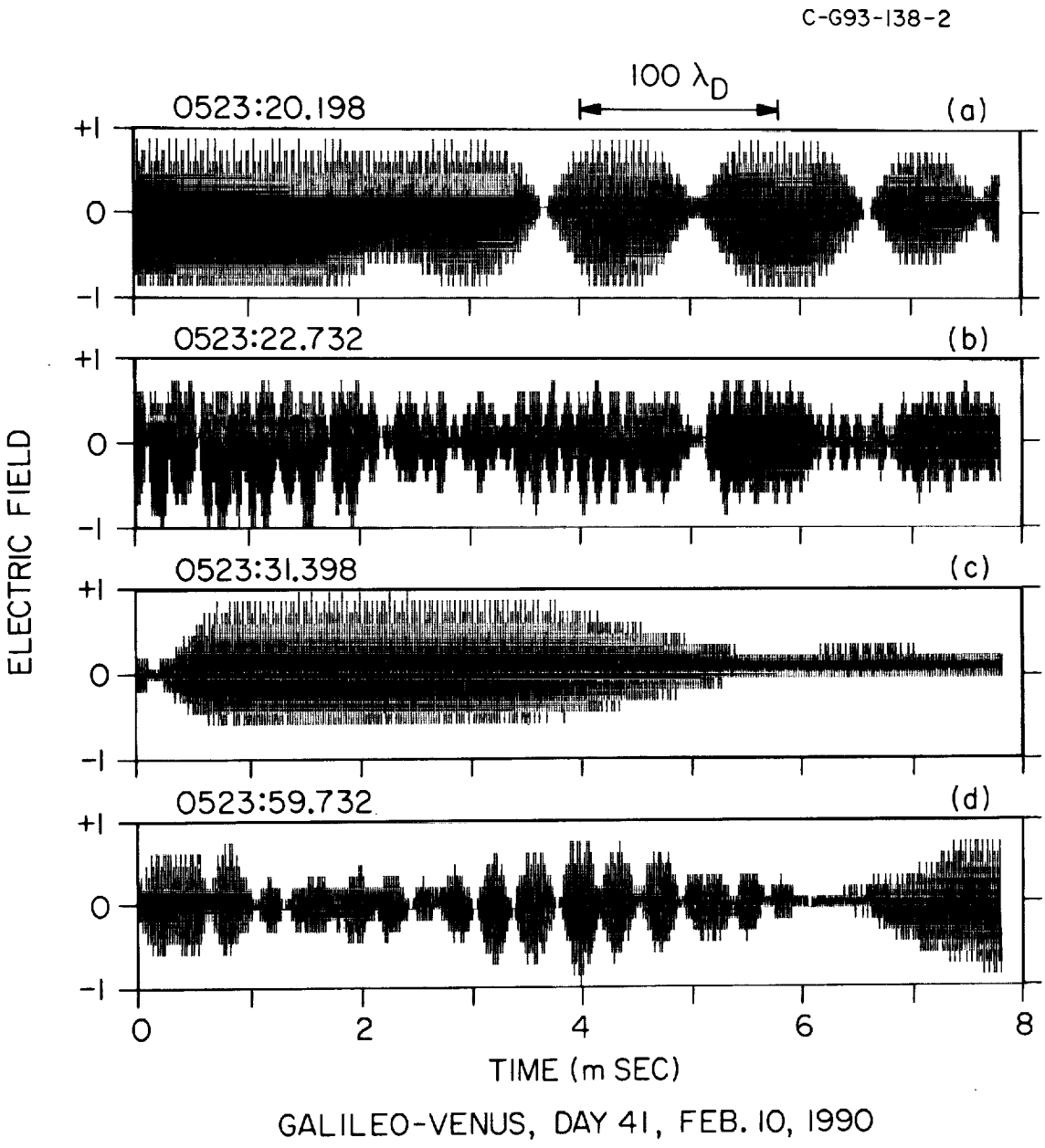
C-G93-138-2
100 λ_D
0523:20.198
(a)
0523:22.732
(b)
0523:31.398
(c)
0523:59.732
(d)
+1
0
-1
ELECTRIC FIELD
0
2
4
6
8
TIME (m SEC)
GALILEO-VENUS, DAY 41, FEB. 10, 1990

Figure 5

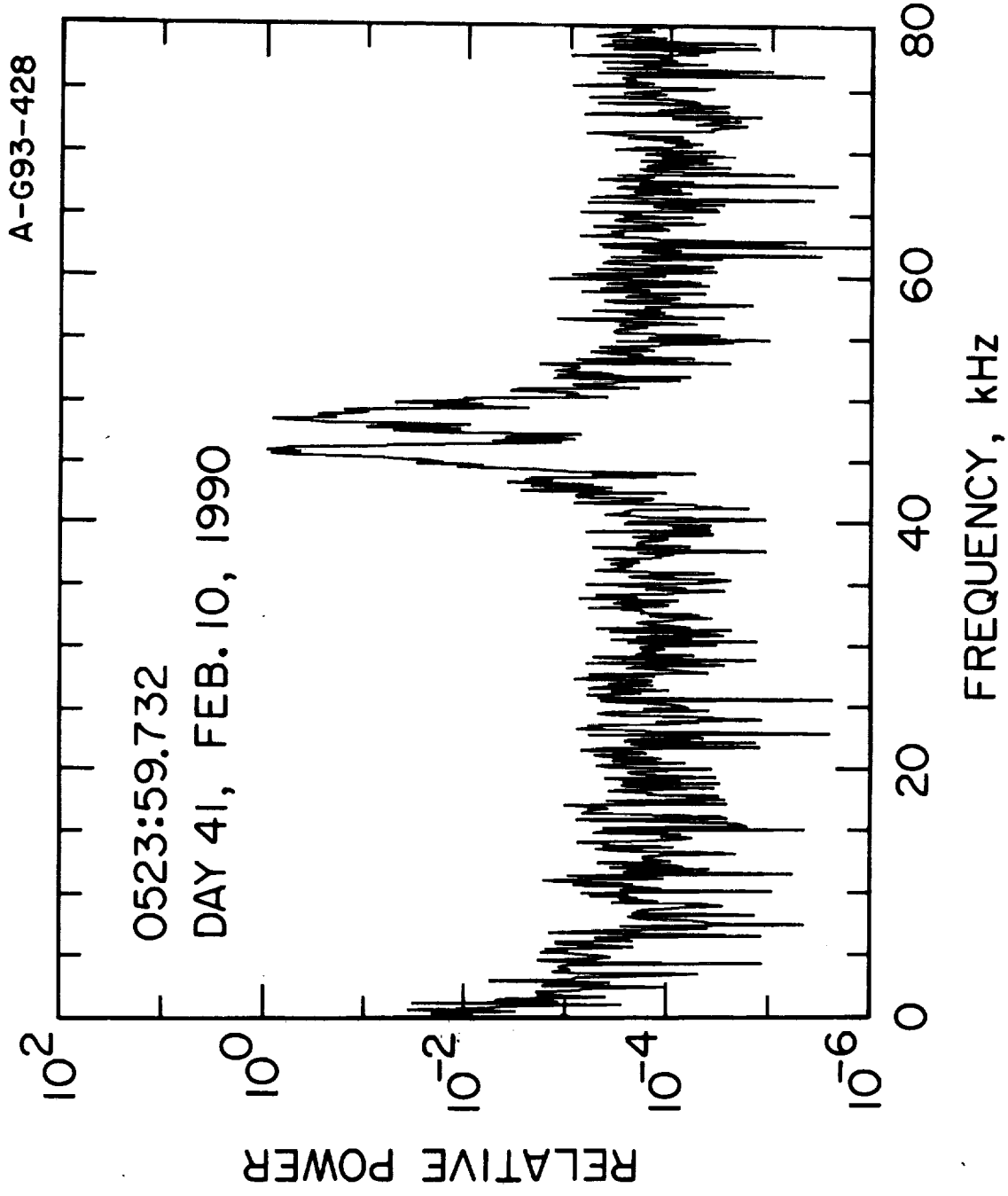
A-G93-428
0523:59.732
DAY 41, FEB. 10, 1990
RELATIVE POWER
10^{2}
10^{0}
10^{-2}
10^{-4}
10^{-6}
0
20
40
60
80
FREQUENCY, kHz

Figure 6

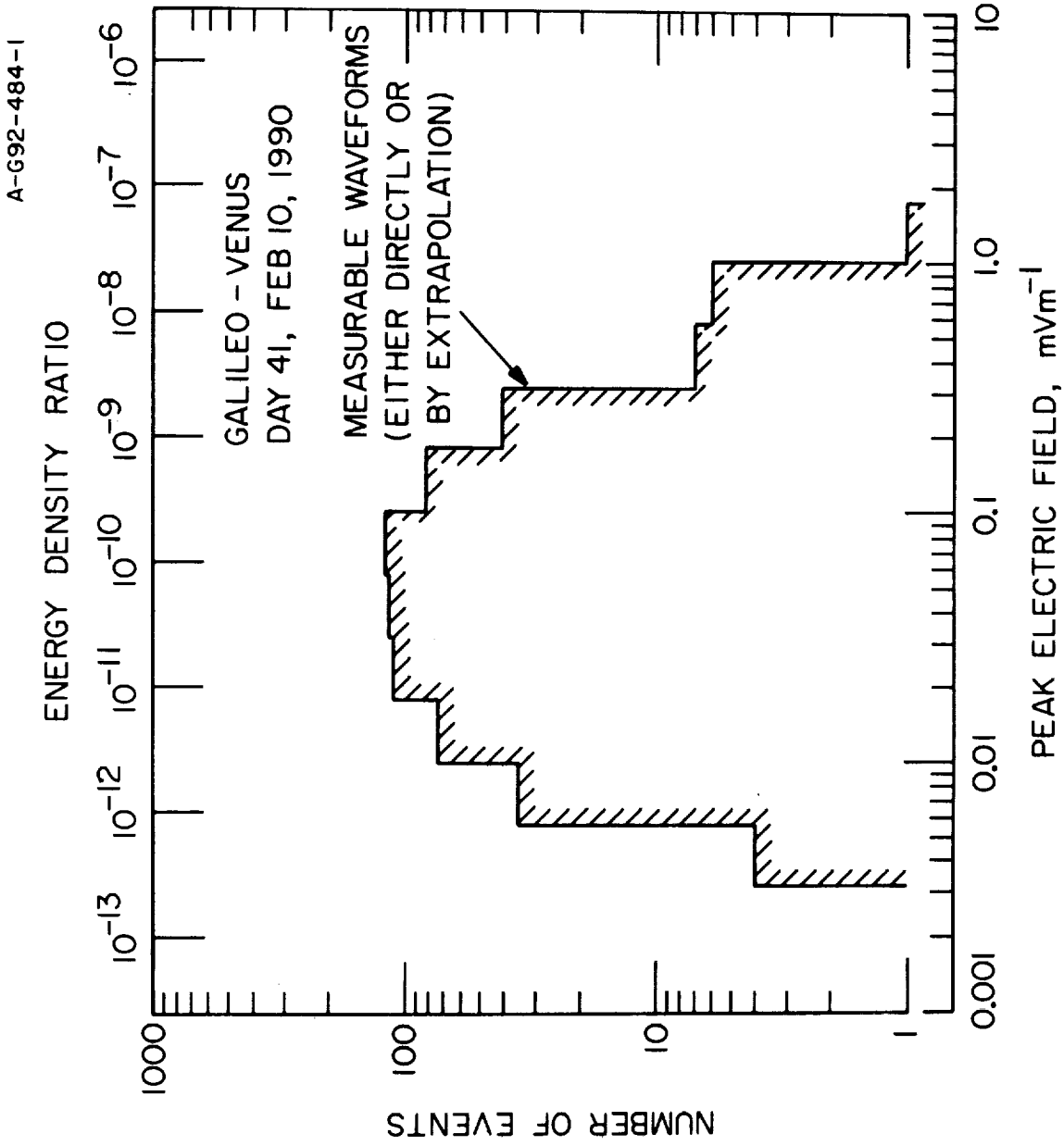
A-G92-484-1
ENERGY DENSITY RATIO
10^{-13}
10^{-12}
10^{-11}
10^{-10}
10^{-9}
10^{-8}
10^{-7}
10^{-6}
GALILEO - VENUS
DAY 41, FEB 10, 1990
MEASURABLE WAVEFORMS
(EITHER DIRECTLY OR
BY EXTRAPOLATION)
NUMBER OF EVENTS
1000
100
10
1
PEAK ELECTRIC FIELD, mVm^{-1}
0.001
0.01
0.1
1.0
10

Figure 7

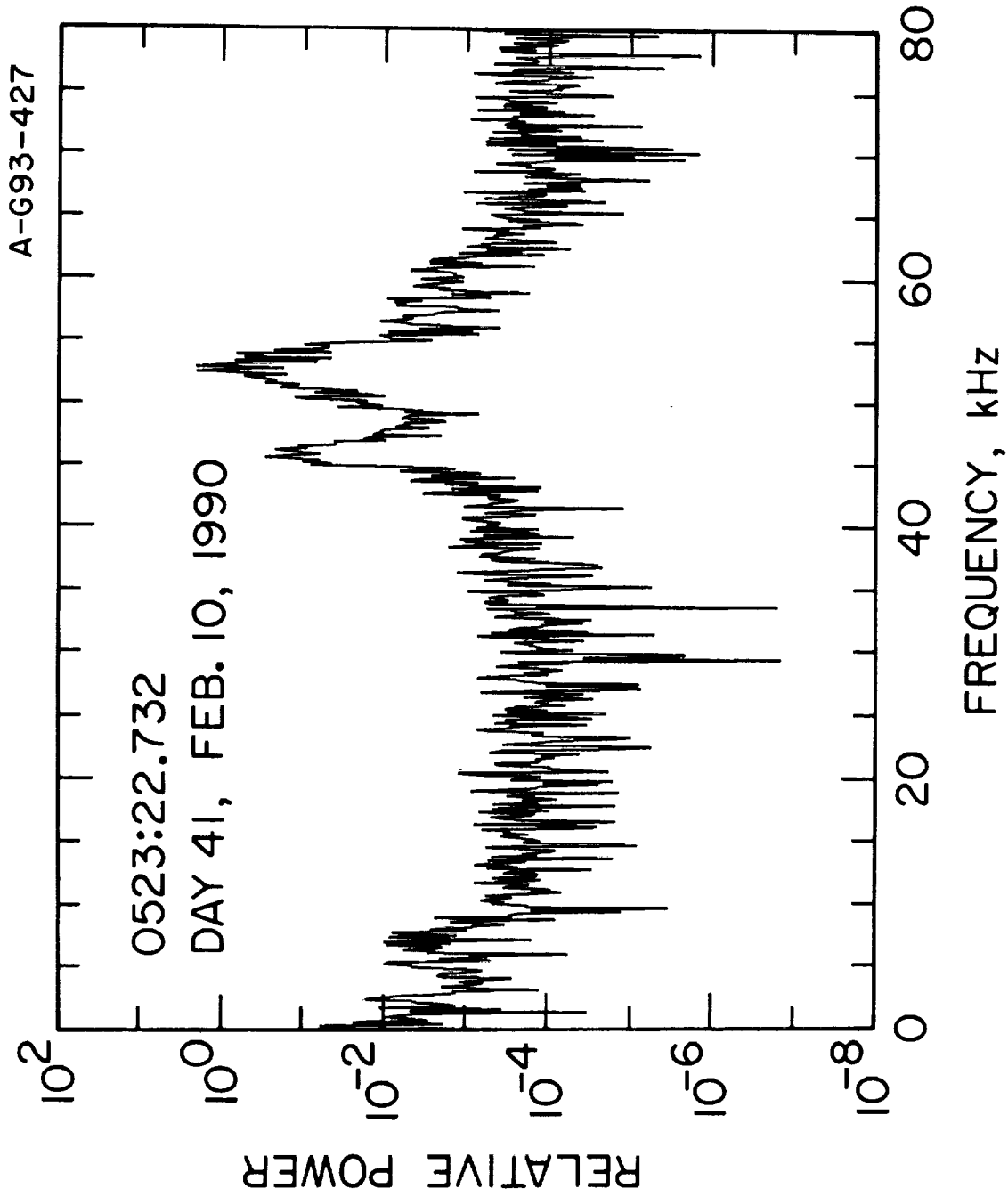
A-G93-427
0523:22.732
DAY 41, FEB. 10, 1990
RELATIVE POWER
FREQUENCY, kHz
10^{2}
10^{0}
10^{-2}
10^{-4}
10^{-6}
10^{-8}
0
20
40
60
80

Figure 8